C–N Bond Cleavage | *Hot Paper*

Esterification of Tertiary Amides: Remarkable Additive Effects of Potassium Alkoxides for Generating Hetero Manganese–Potassium Dinuclear Active Species

Takahiro Hirai,[a] Daiki Kato,[a] Binh Khanh Mai,[b] Shoichiro Katayama,[a] Shoko Akiyama,[a] Haruki Nagae,[a] Fahmi Himo,*[b] and Kazushi Mashima*[a]

Abstract: A catalyst system of mononuclear manganese precursor **3** combined with potassium alkoxide served as a superior catalyst compared with our previously reported manganese homodinuclear catalyst **2a** for esterification of not only tertiary aryl amides, but also tertiary aliphatic amides. On the basis of stoichiometric reactions of **3** and potassium alkoxide salt, kinetic studies, and density functional theory (DFT) calculations, we clarified a plausible reaction mechanism in which in situ generated manganese–potassium heterodinuclear species cooperatively activates the carbonyl moiety of the amide and the OH moiety of the alcohols. We also revealed details of the reaction mechanism of our previous manganese homodinuclear system **2a**, and we found that the activation free energy ($\Delta G^{\ddagger}$) for the manganese–potassium heterodinuclear complex catalyzed esterification of amides is lower than that for the manganese homodinuclear system, which was consistent with the experimental results. We further applied our catalyst system to deprotect the acetyl moiety of primary and secondary amines.

Introduction

Amides are extraordinarily stable because of the resonance contribution between the nitrogen lone pair and the carbonyl. Amides are ubiquitous and abundant, and are often found in natural compounds such as proteins as well as in synthetic organic compounds such as poly(amides) and pharmaceuticals.[1–5] Cleavage of stable amide bonds under mild conditions has attracted the ongoing attention of organic chemists,[6] and rational strategies, such as diminishing the resonance structure of the C–N bond by complexing *N*,*N*-(2-pyridylmethyl)amides with Cu^{II} sources[7,8] and the construction of a twisted structure around the nitrogen atom have been investigated.[9,10] Cleavage of the common amide bond without these complex strategies requires harsh reaction conditions using stoichiometric amounts of strong acids or bases at high temperatures, and produces the corresponding acids via hydrolysis and esters via alcoholysis.

Some metal catalyst systems have been developed for primary and secondary amides. Fisher et al. reported $TiCl_4$-mediated alcoholysis of inactivated primary amides as the first example of metal-catalyzed alcoholysis, but the reaction required 1 equiv of aqueous HCl.[11] We developed a catalytic C–N bond cleavage of secondary *N*-β-hydroxyethylamides mediated by zinc triflate,[12] or primary amides and secondary acetanilide derivatives using a catalyst mixture of $Sc(OTf)_3$ with boronic esters.[13] Atkinson et al. followed up on our work using $Sc(OTf)_3$ for the catalytic esterification of primary amides,[14] and Ohshima et al. recently reported catalytic esterification of 8-aminoquinoline amides achieved by $Ni(tmhd)_2$ (TMHD = 2,2,6,6-tetramethyl-3,5-heptanedionate) in methanol.[15] In addition, Shimizu et al. used cerium dioxide for the catalytic esterification of primary amides, despite its heterogeneity.[16]

With respect to the catalytic transformation of tertiary amides, which are more stable than primary and secondary amides,[17] three mechanisms have been reported including oxidative addition, *N*,*O*-acyl rearrangement, and Lewis acid-assisted mechanisms.[18–27] Oxidative addition-esterification was first reported by Garg and co-workers who used nickel(0) catalysts to activate the C–N bond of tertiary arylamides bearing functional groups such as Ph, Boc, and Ts by oxidative addition as a key step to afford the corresponding aryl esters.[18,19] Danoun and Gosmini used a low-valent cobalt catalyst system supported by 2,2′-bipyridine with metallic manganese as a reductant

[a] T. Hirai, D. Kato, S. Katayama, S. Akiyama, Dr. H. Nagae, Prof. Dr. K. Mashima
Department of Chemistry, Graduate School of Engineering Science
Osaka University, Toyonaka, Osaka 560-8531 (Japan)
E-mail: mashima@chem.es.osaka-u.ac.jp

[b] Dr. B. K. Mai, Prof. Dr. F. Himo
Department of Organic Chemistry, Arrhenius Laboratory
Stockholm University, SE-106 91 Stockholm (Sweden)
E-mail: fahmi.himo@su.se

Supporting information and the ORCID identification number(s) for the author(s) of this article can be found under: https://doi.org/10.1002/chem.202001447.

to catalytically activate the C–N bond of activated arylamides bearing a Boc, Ts, or methoxycarbonyl group to give the corresponding aryl esters.[20] Notably, low-valent nickel and cobalt species oxidatively added to the C–N bond of activated amides bearing functional groups such as Ph, Boc, Ts, and methoxycarbonyl on the nitrogen atom; without these functional groups, no smooth reaction proceeded (Scheme 1 a).[21] For *N*,*O*-acyl rearrangement esterification, we reported two catalyst systems, $Mn(acac)_2$ combined with 2,2′-bipyridine[22] and zinc triflate, that catalyzed the esterification of *N*-alkyl-*N*-β-hydroxyethylamides,[23] although these catalysts required substrates with a β-hydroxyethyl group on the nitrogen atom (Scheme 1 b). For Lewis acid-assisted esterification, $FeCl_3$ required stoichiometric amounts of HCl for the catalytic esterification of tertiary amides,[24] and heterogeneous cerium dioxide required a high temperature (175 °C) for the catalytic esterification of tertiary amides (Scheme 1 c).[25,26]

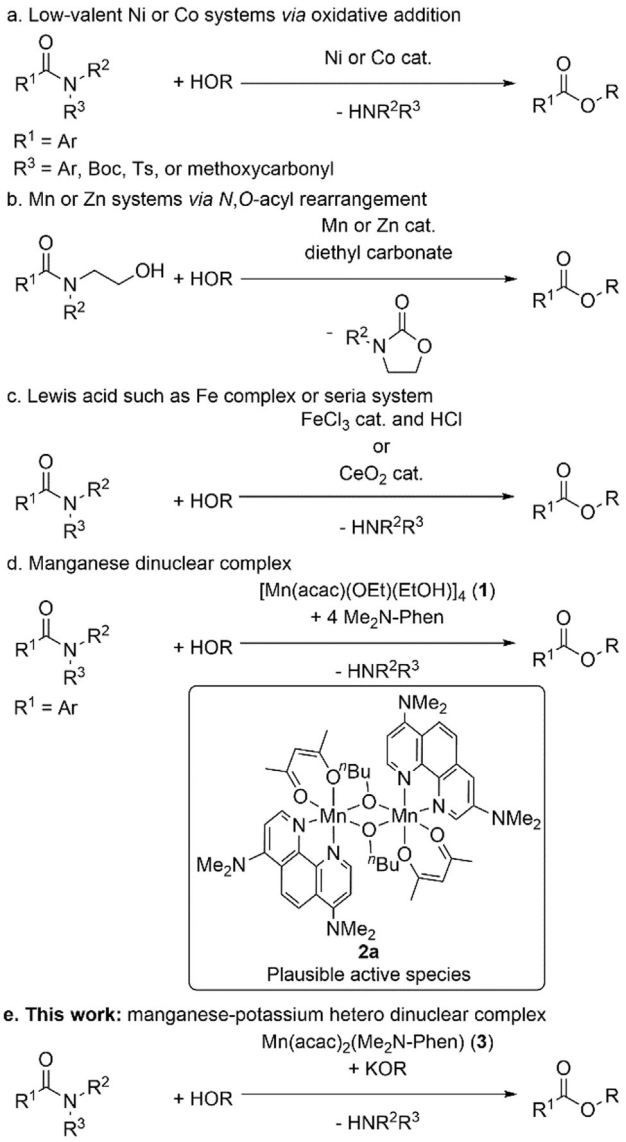

Scheme 1. Catalytic esterification for tertiary amides.

In this context, we focused our attention on developing effective catalysts for the esterification of simple tertiary *N*,*N*-dialkyl amides. We previously found that an alkoxide-bridged manganese dinuclear complex, $[(acac)(Me_2N\text{-}Phen)Mn(\mu\text{-}OnBu)]_2$ (**2 a**) (Me_2N-Phen = 4,7-bis(dimethylamino)-1,10-phenanthroline), derived by treating an alkoxide-bridged manganese tetranuclear cubic complex $[Mn(acac)(OEt)(EtOH)]_4$ (**1**) with Me_2N-Phen in *n*BuOH, was an excellent catalyst for the esterification of various *N*,*N*-dialkyl arylamides via a cooperative mechanism in which one manganese center functioned as a Lewis acid for coordinating to the amide carbonyl moiety and the second manganese center activated an alcohol to provide more nucleophilic alkoxide species (Scheme 1 d).[28] Herein, we report another manganese catalyst system, $Mn(acac)_2(Me_2N\text{-}Phen)$ (**3**), and the remarkable additive effects of potassium alkoxides that improved the catalytic activity of **3** for the esterification of not only *N*,*N*-dialkyl benzamides but also *N*,*N*-dialkyl aliphatic amides. Kinetic studies together with density functional theory (DFT) calculations and mass spectrometry analysis revealed that adding potassium alkoxide to **3** generated a manganese–potassium heterodinuclear species in situ, the catalytic activity of which was superior to that of our previously reported manganese homodinuclear catalyst **2 a** (Scheme 1 e).

Results and Discussion

We began by searching for convenient and more active manganese precursors for the catalytic esterification of *N*,*N*-dimethyl naphthamide (**4 a**) under the conditions of *n*BuOH at 135 °C for 18 h to give the corresponding ester **5 a**, although we previously reported that dinuclear complex **2 a** exhibited sufficient catalytic performance.[28] As the result, we selected $Mn(acac)_3$ (5 mol%) as the best precursor, and we selected 4,7-bisdimethyamino-1,10-phenanthroline (Me_2N-Phen, 5 mol%) as the best chelating ligand [Eq. (1), for more details, see Tables S1–S3]. Under these reaction conditions, the reverse reaction was unfavorable because the byproduct, gaseous dimethylamine, was easily discharged from the reaction mixture.

Figure 1 (plots of ●) shows the reaction profile for the catalyst system of $Mn(acac)_3$/Me_2N-Phen, revealing a rather long induction period (ca. 30–40 min) due to the reduction from Mn^{III} to Mn^{II} at the initiation stage. Accordingly, we conducted a stoichiometric reaction with $Mn(acac)_3$ and Me_2N-Phen in *i*PrOH at reflux temperature for 24 h to give a Mn^{II} complex, $Mn(acac)_2(Me_2N\text{-}Phen)$ (**3**), in 65% yield, which was characterized by mass spectrometry ($[\mathbf{3}]^+$ $m/z = 519.18$) and by X-ray analysis (Figure 2) given its paramagnetic nature. When isolated complex **3** was used as the catalyst, the induction period was shorter (ca. 10 min, Figure 1, plots of ◆). A notable finding was that the reaction rate of **3** was almost equal to that of dinuclear complex **2 a** derived in situ from the tetranuclear cubic

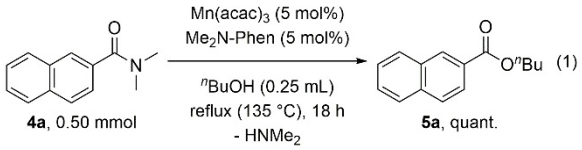

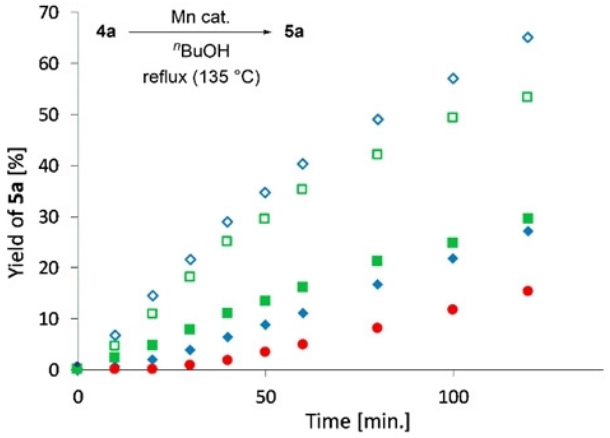

Figure 1. Time course of the catalytic esterification of **4a** (2.0 M) in *n*BuOH by manganese catalyst systems (100 mM, 5 mol%); $Mn(acac)_3$+Me_2N-Phen (●), **3** (◆), **2a** (■), **3**+KOMe (◇), **2a**+KOMe (□).

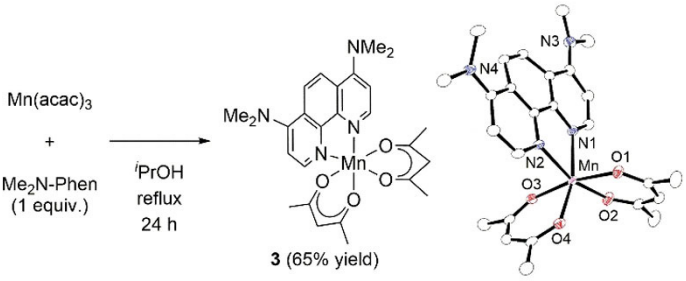

Figure 2. Synthesis and crystal structure of **3** with 50% thermal ellipsoids. All hydrogen atoms and solvent molecule are omitted for clarity. Selected bond lengths (Å) and bond angles (degree): Mn–N1 2.2519(12), Mn–N2 2.2716(13), Mn–O1 2.1799(11), Mn–O2 2.1519(12), Mn–O3 2.1462(11), Mn–O4 2.1571(10); N1-Mn-N2 71.94(5), O1-Mn-O2, 83.08(4), O3-Mn-O4, 83.54(4).

complex **1** and Me_2N-Phen in *n*BuOH (Figure 1, plots of ■), indicating that the short induction period was due to the formation of **2a** from **3** in *n*BuOH. When **3** was dissolved in EtOH (0.065 mM), its UV/Vis spectrum did not change at room temperature; however, at 70 °C, the absorption band of **3** (λ_{max} = 298 nm) decreased and the new absorption band at 343 nm increased with an isosbestic point at 319 nm (Figure S2). The new absorption band was assigned to the homodinuclear complex [(acac)(Me_2N-Phen)Mn(μ-OEt)]$_2$ (**2b**), which was alternatively prepared by treating [Mn(acac)(OEt)(EtOH)]$_4$ (**1**) with Me_2N-Phen in EtOH.[28]

To our surprise, KOMe (1 equiv) exhibited remarkable additive effects with **3** (Figure 1, plots of ◇), which not only decreased the induction period, but also improved its catalytic activity compared with **2a** as well as **3** without any additives. Moreover, the reaction profile of **2a** with 1 equiv of KOMe (Figure 1, plots of □) was almost the same as that of **3** with 1 equiv of KOMe (Figure 1, plots of ◇). The catalytic activity of KOMe alone was quite low, and almost no catalytic activity of KOMe was observed after 30 min. In addition, the yield of **5a** catalyzed by a mixture of **3** and KOMe was significantly higher than the combined yields of **5a** catalyzed by either **3** or KOMe alone for the entire reaction time (see the Supporting Information for details). These results suggest that manganese complex **3** and KOMe cooperatively catalyzed the esterification of **4a**. When the reaction mixture of **3** and 1 equiv of KOMe in EtOH was heated at 70 °C, **3** (298 nm) was rapidly consumed and absorbance at 343 nm was increased (Figure S3). Although the obtained spectra were the same as for **2a**, electrospray ionization time-of-flight mass spectrometry of the resulting solution revealed a parent peak at m/z = 686.29, which was assigned to a manganese–potassium heterodinuclear species $[(Me_2N\text{-Phen})(acac)Mn(OEt)_3K(EtOH)_2]^+$, in which the manganese center was two-electron oxidized during the measurements (Figure S4). As a result, we concluded that the addition of KOMe (1 equiv) had dual functions to induce the formation of dinuclear manganese complex **2a** from **3** in *n*BuOH and to generate a manganese–potassium heterodinuclear complex, $(Me_2N\text{-Phen})(acac)Mn(\mu\text{-}OMe)_2K(solvent)_n$ (**6**), as a more catalytically active species (see below). Finally, we selected the in situ mixture of **3** and KOMe (1 equiv) as the best catalyst system.

With regard to the additives, we further optimized the alkoxides of alkaline metals under the conditions using **3** (5 mol%) at reflux temperature in *n*BuOH; the results are shown in Table 1. The addition of 1 equiv of KOMe gave **5a** in 44% yield after 1 h (entry 1), and 96% yield after 12 h (entry 2). Another potassium alkoxide salt, $KOCH_2C_6H_4(4\text{-}CH_3)$, exhibited almost the same catalytic performance as that of KOMe, giving **5a** in 46% yield for 1 h (entry 3), and 95% yield for 12 h (entry 4), whereas KOPh resulted in less activity, giving **5a** in 24% yield after a 1 h reaction (entry 5). Reaction with LiOMe and NaOMe for 1 h afforded **5a** in 21% and 39% yield, respectively (entries 6 and 7), suggesting that a large alkali metal showed higher catalytic activity. Without any additives, **4a** was converted into **5a** in 1 h in only 17% yield (entry 8). Therefore, we selected two potassium alkoxides, KOMe and $KOCH_2C_6H_4(4\text{-}CH_3)$, as suitable additives.

Table 1. Additive effects of alkaline alkoxides to **3**.

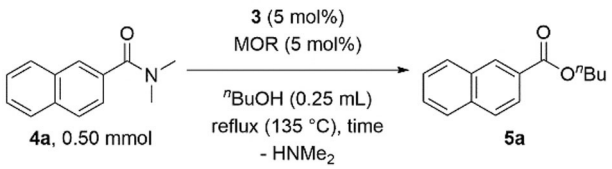

Entry	MOR	Time [h]	Yield [%][a]
1	KOMe	1	44
2	KOMe	12	96 (90)
3	$KOCH_2C_6H_4(4\text{-}CH_3)$	1	46
4	$KOCH_2C_6H_4(4\text{-}CH_3)$	12	95
5	KOPh	1	24
6	LiOMe	1	21
7	NaOMe	1	39
8	none	1	17

[a] Determined by GC analysis with dodecane as internal standard. Isolated yield is given in parentheses.

Kinetics of the catalyst system comprising 3 and $KOCH_2C_6H_4(4\text{-}CH_3)$

We measured the reaction rate in relation to the concentration of amide **4a** and catalyst **3** upon activation by $KOCH_2C_6H_4(4\text{-}CH_3)$ (1 equiv to **3**) in *n*BuOH, and observed first-order rate dependence on the concentration of amide **4a** (Figure 3) and half-order rate dependence on the concentration of **3** over a 3-fold range (Figure 4) when we applied a normalized timescale method;[29,30] the velocity accordingly obeys $k_{obs}[\mathbf{3}]^{0.5}[\mathbf{4a}]^{1}$. The half-order rate dependency of **3** suggested that a mixed metal dormant species **D**, containing manganese and potassium atoms, was in equilibrium between a catalytic active species **6** generated in situ from **3**, KOMe, and an acetylacetone liberated from **3**.[31] We thus estimated the activation parameters using Eyring plots, and $\Delta H^{\ddagger}$, $\Delta S^{\ddagger}$, and $\Delta G^{\ddagger}$ at 135 °C were calculated as 15.9 ± 0.5 kcal mol^{-1}, -157 ± 5 J mol^{-1}·K^{-1}, and 31.2 ± 1.0 kcal mol^{-1}, respectively (Figure 5, plots of ●). The $\Delta G^{\ddagger}$ at 135 °C of the esterification catalyzed by **3** with potassium salt was smaller than that of the esterification catalyzed by **2a** ($\Delta G^{\ddagger} = 32.6 \pm 1.5$ kcal mol^{-1} at 135 °C, Figure 5, plots of ■). The large negative $\Delta S^{\ddagger}$ value suggests that the rate-determining step is the nucleophilic attack of the alkoxide moiety to the amide carbonyl moiety, in which three components (catalyst, amide, and alcohol) are involved to form a highly ordered transition state.

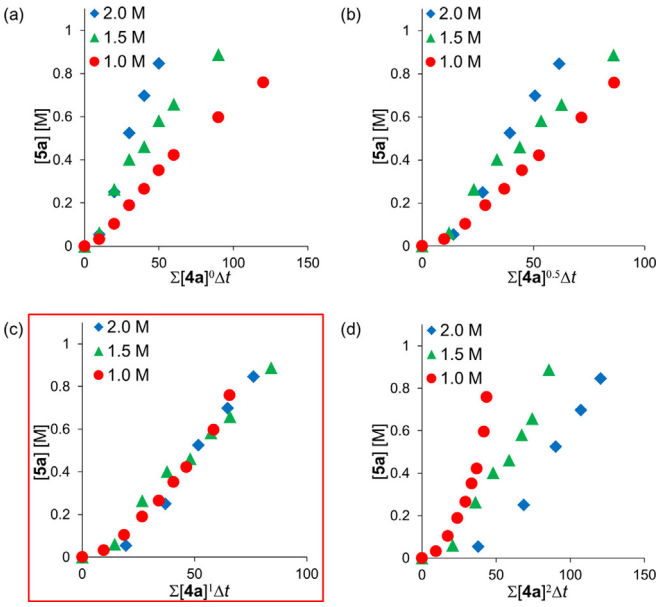

Figure 3. Normalized timescale analysis to determine the order in amide **4a**: a) $\alpha = 0$, b) $\alpha = 0.5$, c) $\alpha = 1.0$, d) $\alpha = 2.0$.

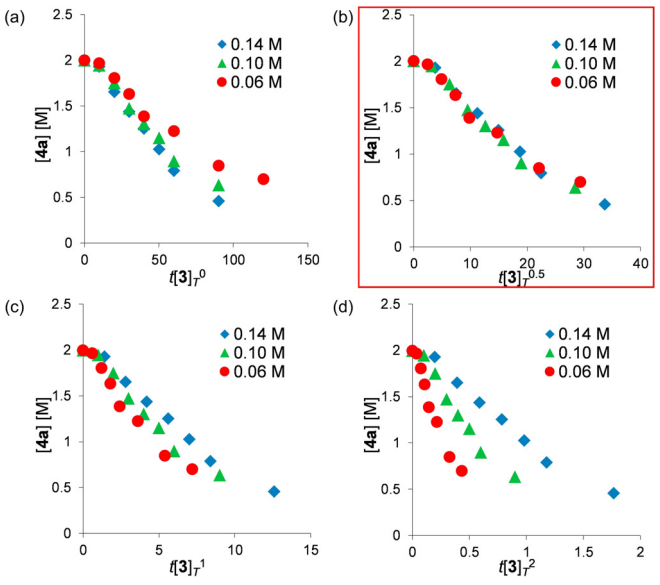

Figure 4. Normalized timescale analysis o to determine the order in catalysts **3**; a) $n = 0$, b) $n = 0.5$, c) $n = 1.0$, d) $n = 2.0$.

Simulated mechanism by DFT calculations

To shed more light on the mechanism of this novel esterification and on the role of potassium alkoxide, DFT calculations were performed with the dispersion-corrected B3LYP functional using *N*,*N*-dimethyl-2-naphthamide (**4a**) as a representative substrate.[28,32]

The catalytic cycle of the esterification of **4a** by manganese homodinuclear complex **2a** is shown in Figure 6a. The first step of the catalytic cycle is the coordination of **4a** to a manganese center and the dissociation of one μ-O*n*Bu bridge to form a terminal alkoxide giving **int1-Mn$_2$** which was calculated to be 15.1 kcal mol^{-1} higher than **2a** (Figure 6c). The terminal alkoxide then performs a nucleophilic attack at a carbonyl moiety of the **4a** via transition state **TS1-Mn$_2$** (Figure 6e), generating a bridging alkoxide intermediate, **int2-Mn$_2$**. The activation energy of **TS1-Mn$_2$** is calculated to be 32.2 kcal mol^{-1} relative to the starting point at **2a**, and intermediate **int2-Mn$_2$** was +24.7 kcal mol^{-1}. To proceed, we found that the reaction required another *n*BuOH molecule to obtain reasonable energy barriers. The coordination of one *n*BuOH to one manganese center affords **int3-Mn$_2$**, in which the bridging *tert*-alkoxide becomes terminal. A proton is transferred from the coordinating *n*BuOH to the amino moiety of the *tert*-alkoxide, together with C–N bond cleavage via transition state **TS2-Mn$_2$** (Figure 6f). The calculated barrier for this concerted C–N bond cleavage step is 32.9 kcal mol^{-1} relative to **2a**. The ester **5a** and the dimethylamine by-product are released in this step, and the manganese homodinuclear complex **2a** is regenerated. The overall reaction was calculated to be slightly exergonic, by 1.8 kcal mol^{-1}. The calculated barriers of this mechanism are consistent with the experimental result, $\Delta G^{\ddagger} = 32.6 \pm 1.5$ kcal mol^{-1} (see above). Given that the energies of **TS1-Mn$_2$** and **TS2-Mn$_2$** were very close (32.2 and 32.9 kcal mol^{-1}, respectively), the rate-determining step cannot be confidently determined on the basis of these calculations alone. Previous kinetic experiments, however, indicated that the initial nucleophilic attack is the rate-determining step.[28] It should be noted that a transition state for C–N bond cleavage without participation of the additional *n*BuOH (**TS2′-Mn$_2$**) was also considered, but the

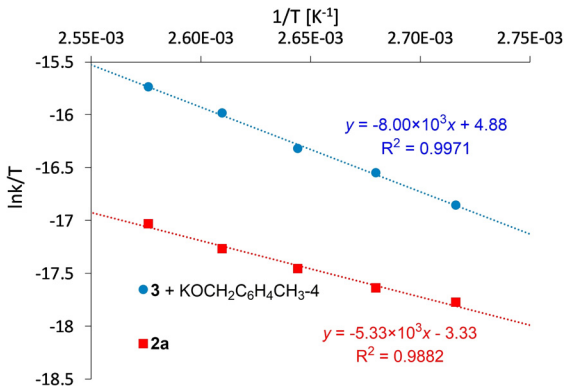

Figure 5. Eyring plots for the esterification of **4a** catalyzed by a catalyst mixture of **3** and $KOCH_2C_6H_4(4\text{-}CH_3)$ (1 equiv to **3**), and **2a**.

obtained energy barrier was very high, thus ruling out this possibility.[32]

Next, we turned our efforts to rationalize the role of the potassium alkoxide in this novel esterification. We found that **3**, $KOCH_2C_6H_4(4\text{-}CH_3)$, and *n*BuOH are reacted to form manganese–potassium heterodinuclear alkoxylate complex **6**, in which one of two acetylacetonate ligand of **3** dissociates to give an acetylacetone (Figure 6b). This process is calculated to be exergonic by 2.6 kcal mol^{-1}. The complex **6** is reacted with 1 equiv of acetylacetone, which derives from **3**, to give a dormant species **D**. The dormant species **D** is more stable than **6** by 1.3 kcal mol^{-1}, a value that indicates that complexes **6** and **D** are in equilibrium in the catalytic cycle. The calculations show that, starting from **6**, the catalytic cycle follows the same steps as in the case of the dinuclear manganese complex. The barriers for the nucleophilic attack (**TS1-MnK**) and C–N bond cleavage (**TS2-MnK**), however, were calculated to be lower in energy, 29.6 and 31.4 kcal mol^{-1}, respectively (Figure 6d), similar to the results of the Eyring plots ($\Delta G^{\ddagger} = 31.2 \pm 1.0$ kcal mol^{-1}, see above). This finding was due mainly because the energetic penalty associated with the binding of the substrate to the catalyst was lower in the case of manganese–potassium heterodinuclear complex (12.0 kcal mol^{-1}) compared with manganese homodinuclear complex (15.1 kcal mol^{-1}). The lower barriers obtained by adding potassium alkoxide is consistent with the experimental observations.

Substrate scope

We next screened the substrate scope on several *N*,*N*-dimethyl aliphatic amides, which are more stable than *N*,*N*-dimethylbenzamide,[17] making it difficult to apply our previous manganese homodinuclear system (Table 2).[28] *N*,*N*-Dimethyl-3-phenylpropionamide (**7a**) was converted into butyl 3-phenylpropionate (**8a**) in 92% yield by using the combined catalyst system of **3** and KOMe (entry 1); this yield is higher than the combined yields of **7a** catalyzed separately by **3** and KOMe (see the Supporting Information for details). *N*,*N*-Dimethyl-3-(*p*-tolyl)propanamide (**7b**), 3-(4-methoxyphenyl)-*N*,*N*-dimethylpropanamide (**7c**), and *N*,*N*-dimethyl-3-(4-(trifluoromethyl)-phenyl)propanamide (**7d**) exhibited almost the same reactivity as **8a**, giving the corresponding esters **8b**, **8c**, and **8d** in 86, 88, and 94% yield, respectively (entries 2–4). *N*,*N*-Dimethyl-4-phenylbutanamide (**7e**), which has a longer alkyl chain than **7a**, had slightly lower reactivity, giving butyl 4-phenylbutanonate (**8e**) in 79% yield (entry 5). When the reaction time was extended to 45 h, however, **8e** was produced in 84% yield (entry 6). Aliphatic amides bearing a C=C double bond such as *N*,*N*-dimethylcinnamamide (**7f**) provided the corresponding ester **8f** in 95% yield without any loss of the olefin moiety (entry 7). *N*,*N*,2-Trimethyl-3-propanamide (**7g**) gave only a trace amount of ester **8g**, due to the steric hindrance around the carbonyl moieties (entry 8). We also investigated the substrate scope of several *N*,*N*-dimethylbenzamide derivatives, and found that each substrate gave almost the same yield of the corresponding butyl benzoate derivatives as that of the previously developed manganese homodinuclear system **2a** (Table S6).[32]

3-Phenyl propionamides of various amines required the addition of one equivalent of diethyl carbonate to trap the eliminating amines (Table 3). In the presence of diethyl carbonate (1 equiv), piperidine and morpholine derivatives **9a** and **9b** gave **8a** in 74 and 77% yields, respectively (entries 1 and 2). *N*-Methyl-*N*,3-phenyl-propanamide **9c** was converted into **8a** in 91% yield (entry 3). *N*,*N*-Diethyl-3-phenylpropanamide (**9d**), however, afforded no product and all the substrate was recov-

Table 2. Scope and limitation of acyl moieties.

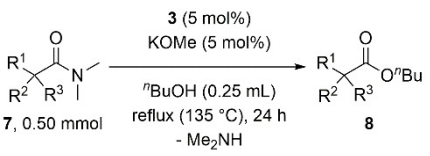

Entry	Substrate (**7**)		Yield of **8** [%][a]
1	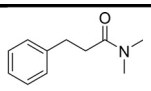	**7a**	**8a** 92
2	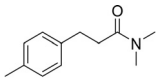	**7b**	**8b** 86
3	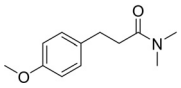	**7c**	**8c** 88
4	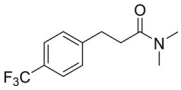	**7d**	**8d** 94
5	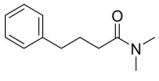	**7e**	**8e** 79
6[b]			**8e** 84
7	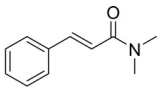	**7f**	**8f** 95
8	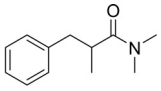	**7g**	**8g** trace[c]

[a] Yield of isolated product. [b] Reaction time was 45 h. [c] Determined by ^{1}H NMR spectroscopic analysis of the crude reaction mixture.

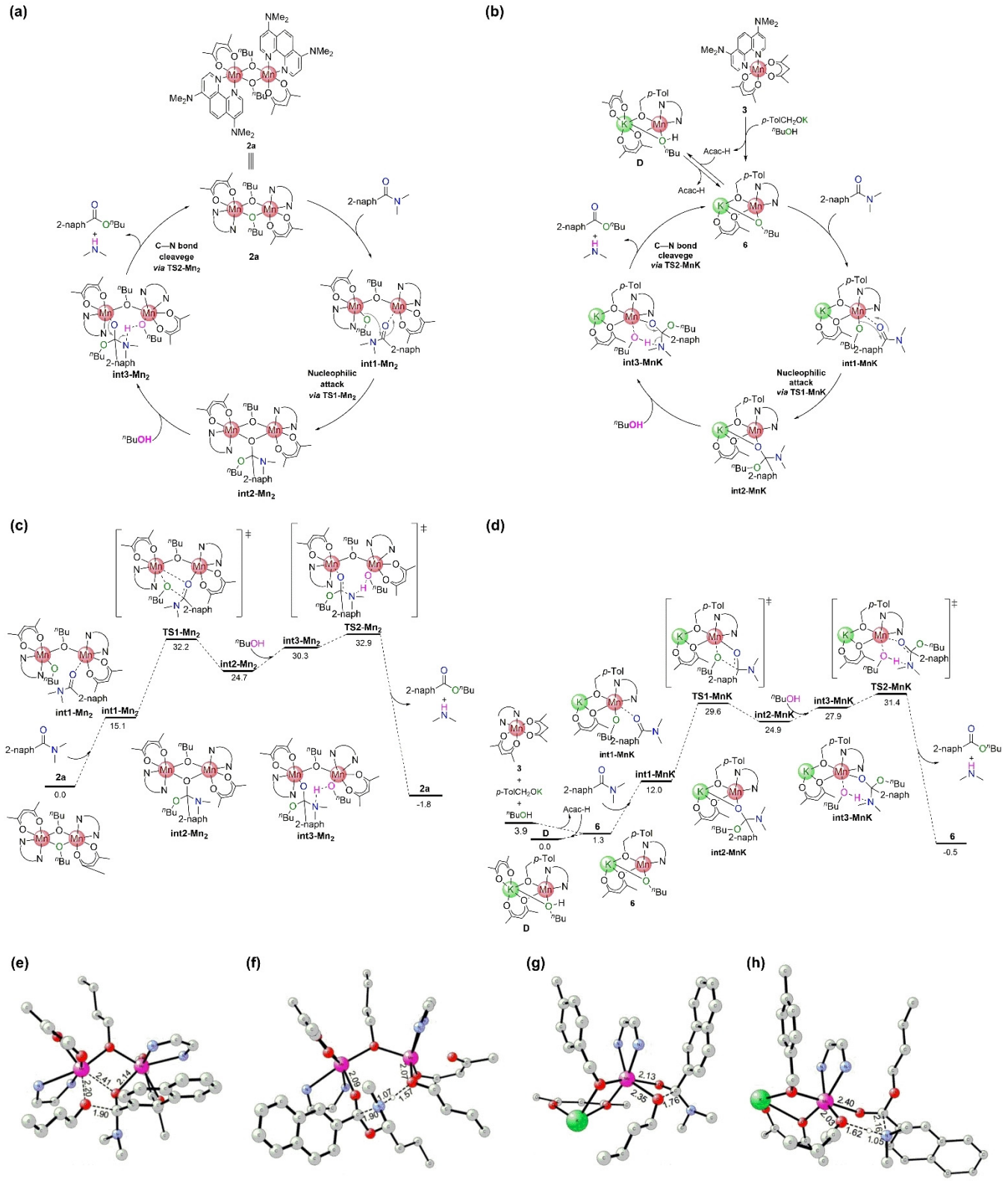

Figure 6. a) Proposed reaction mechanism for the catalysis with manganese homodinuclear complex **2a**. b) Proposed reaction mechanism for catalysis with the manganese–potassium heterodinuclear complex **6**. c) Calculated free energy profile (kcal mol^{-1}) for the catalytic esterification mediated by the manganese homodinuclear complex **2a**. d) Calculated free energy profile (kcal mol^{-1}) for the catalytic esterification mediated by the manganese–potassium heterodinuclear complex **6**. e–h) Optimized structures of transition states **TS1-Mn$_2$**, **TS2-Mn$_2$**, **TS1-MnK**, and **TS2-MnK** for the each homo- and heterodinuclear manganese-catalyzed esterification. Most hydrogen atoms and parts of the *N*,*N*-bidentate ligands are omitted for clarity. Bond lengths are given in Å.

ered, probably due to the steric hindrance around the carbonyl moiety (entry 4). This reaction was applied to secondary and primary amides: *N*-methyl-3-phenyl propanamide (**9e**) and 3-phenyl-*N*-(8-quinolinyl) propanamide (**9f**) afforded **8a** in 75% and 96% yield, respectively, whereas 3-phenyl propanamide (**9g**) afforded **8a** in 78% yield (entries 5–7).

We applied this catalytic system to the deacetylation of acetyl amides of various amines (Table 4). Deacetylation of *N*-methylacetanilide derivatives **10a**, **10b**, and **10c** proceeded smoothly to give the corresponding *N*-methylanilines **11a**, **11b**, and **11c** in 86, 63, and 60% yield, respectively (entries 1–3). Secondary 4-metylacetanilide **10d** was deacetylated in 63% yield (entry 4). In the case of **10e**, with both acetyl and pivaloyl groups, the acetyl moiety was selectively deprotected to give **11e** in 73% yield (entry 5).

Conclusions

We developed a new, efficient catalyst system comprising manganese complex **3** in combination with KOMe for esterification of tertiary aromatic and aliphatic amides, the latter of which has not been successfully achieved previously. We clarified the remarkable additive effects of potassium alkoxide salt to **3** for increasing catalytic activity. The in situ generation of manganese–potassium heterodinuclear species **6** was elucidated by mass spectrometry as well as kinetic studies and DFT calculations. We further applied this catalytic system to the deacetylation of acetyl amides including several primary and secondary amides. These results provide insight into the use of homo- and heterodinuclear manganese metals at the active sites of metalloenzymes that regulate the metabolism of carboxylic acid derivatives in Nature. Further studies by using other base metals for various transformations of carboxylic acid derivatives are ongoing in our laboratory.

Table 3. Scope and limitations of *N,N*-substituted aliphatic amides.

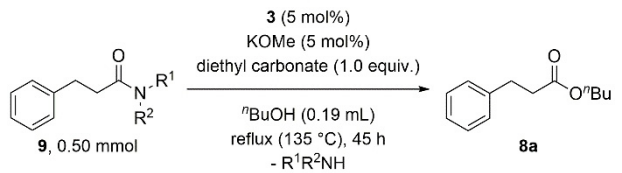

Entry	Substrate (**9**)		Yield of **8a** [%][a]
1	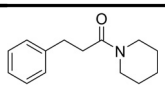	**9a**	74
2	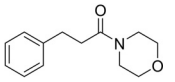	**9b**	77
3	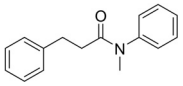	**9c**	91
4	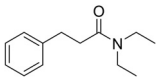	**9d**	n.d.[b]
5	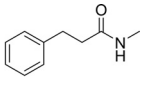	**9e**	75
6	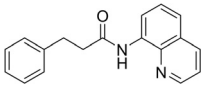	**9f**	96
7	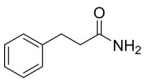	**9g**	78

[a] Determined by ^{1}H NMR spectroscopic analysis with phenanthroline as internal standard. [b] Not detected.

Table 4. Deacetylation of amine moieties.

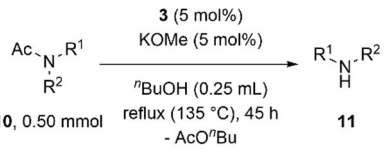

Entry	Substrate (**10**)		Yield of **11** [%][a]
1	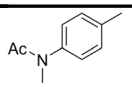	**10a**	**11a** 86
2	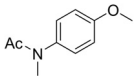	**10b**	**11b** 63
3	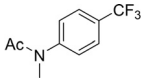	**10c**	**11c** 60
4	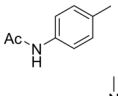	**10d**	**11d** 63
5	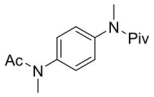	**10e**	**11e** 73

[a] Yield of isolated product.

Acknowledgements

This work was supported by JSPS KAKENHI JP15H05808, JP15K21707, and 20K152770 as a Grant-in-Aid for Scientific Research on Innovative Areas, Precisely Designed Catalysts with Customized Scaffolding (No. 2702), and Grant-in-Aid for Young Scientists. H.N. acknowledges the Toyota Physical and Chemical Research Institute, and Mitsubishi Chemical Award in Synthetic Organic Chemistry, Japan. T.H. acknowledges the JSPS Research Fellowship for Young Scientists for financial support.

Conflict of interest

The authors declare no conflict of interest.

Keywords: amides · reaction mechanisms · reaction intermediates · esterification · manganese

[1] A. Greenberg, C. M. Berneman, J. F. Liebman, *The Amide Linkage: Structural Significance in Chemistry and Biochemistry and Materials Science*, Wiley, New York, **2003**.

[2] H. Lundberg, F. Tinnis, N. Selander, H. Adolfsson, *Chem. Soc. Rev.* **2014**, *43*, 2714 – 2742.
[3] J. M. García, F. C. García, F. Serna, J. L. de la Peña, *Prog. Polym. Sci.* **2010**, *35*, 623 – 686.
[4] R. Das, G. S. Kumar, M. Kapur, *Eur. J. Org. Chem.* **2017**, 5439 – 5459.
[5] S. A. Glover, A. A. Rosser, *J. Org. Chem.* **2012**, *77*, 5492 – 5502.
[6] K. Mashima, Y. Nishii, H. Nagae, *Chem. Rec.* **2020**, *20*, 332 – 343.
[7] R. P. Houghton, R. R. Puttner, *J. Chem. Soc. Chem. Commun.* **1970**, 1270 – 1271.
[8] M. C. Bröhmer, S. Mundinger, S. Bräse, W. Bannwarth, *Angew. Chem. Int. Ed.* **2011**, *50*, 6175 – 6177; *Angew. Chem.* **2011**, *123*, 6299 – 6301.
[9] a) W. E. Doering, J. D. Chanley, *J. Am. Chem. Soc.* **1946**, *68*, 586 – 588; b) H. von Pracejus, M. Kehlen, H. Kehlen, H. Matschiner, *Tetrahedron* **1965**, *21*, 2257 – 2270; c) M. Denzer, H. Ott, *J. Org. Chem.* **1969**, *34*, 183 – 187; d) Y. Arata, T. Kobayashi, *Chem. Pharm. Bull.* **1972**, *20*, 325 – 329; e) H. K. Hall, Jr., R. G. Shaw, A. Deutschmann, *J. Org. Chem.* **1980**, *45*, 3722 – 3724; f) A. J. Bennet, Q.-L. Wang, H. Slebocka-Tilk, V. Somayaji, R. S. Brown, *J. Am. Chem. Soc.* **1990**, *112*, 6383 – 6385; g) N. H. Werstiuk, R. S. Brown, Q. Wang, *Can. J. Chem.* **1996**, *74*, 524 – 532; h) A. J. Kirby, I. V. Komarov, N. Feeder, *J. Am. Chem. Soc.* **1998**, *120*, 7101 – 7102; i) A. J. Kirby, I. V. Komarov, P. D. Wothers, N. Feeder, *Angew. Chem. Int. Ed.* **1998**, *37*, 785 – 786; *Angew. Chem.* **1998**, *110*, 830 – 831; j) A. J. Kirby, I. V. Komarov, N. Feeder, *J. Chem. Soc. Perkin Trans. 2* **2001**, 522 – 529; k) J. Aszodi, D. A. Rowlands, P. Mauvais, P. Collette, A. Bonnfoy, M. Lampilas, *Bioorg. Med. Chem. Lett.* **2004**, *14*, 2489 – 2492; l) M. Szostak, L. Yao, J. Aubé, *J. Org. Chem.* **2009**, *74*, 1869 – 1875; m) F. Macleod, S. Lang, J. A. Murphy, *Synlett* **2010**, 529 – 534; n) M. Hutchby, C. E. Houlden, M. F. Haddow, S. N. G. Tyler, G. C. Lloyd-Jones, K. I. Booker-Milburn, *Angew. Chem. Int. Ed.* **2012**, *51*, 548 – 551; *Angew. Chem.* **2012**, *124*, 563 – 566.
[10] For reweiw, see: M. Szostak, J. Aubé, *Chem. Rev.* **2013**, *113*, 5701 – 5765.
[11] L. E. Fisher, M. J. Caroon, S. R. Stabler, S. Lundberg, S. Zaidi, C. M. Sorensen, M. L. Sparacino, J. M. Muchowski, *Can. J. Chem.* **1994**, *72*, 142 – 145.
[12] Y. Kita, Y. Nishii, T. Higuchi, K. Mashima, *Angew. Chem. Int. Ed.* **2012**, *51*, 5723 – 5726; *Angew. Chem.* **2012**, *124*, 5821 – 5824.
[13] Y. Kita, Y. Nishii, A. Onoue, K. Mashima, *Adv. Synth. Catal.* **2013**, *355*, 3391 – 3395.
[14] B. N. Atkinson, J. M. J. Williams, *Tetrahedron Lett.* **2014**, *55*, 6935 – 6938.
[15] a) T. Deguchi, H.-L. Xin, H. Morimoto, T. Ohshima, *ACS Catal.* **2017**, *7*, 3157 – 3161; b) H. Morimoto, W. Akksd, T. Deguchi, T. Ohshima, *Heterocycles* **2020**, *101*, 471 – 485.
[16] S. M. A. H. Siddiki, A. S. Touchy, M. Tamura, K. Shimizu, *RSC Adv.* **2014**, *4*, 35803 – 35807.
[17] I. I. Marochkin, O. V. Dorofeeva, *Comput. Theor. Chem.* **2012**, *991*, 182 – 191.
[18] L. Hie, N. F. Fine Nathel, T. K. Shah, E. L. Baker, X. Hong, Y.-F. Yang, P. Liu, K. N. Houk, N. K. Garg, *Nature* **2015**, *524*, 79 – 83.
[19] L. Hie, E. L. Baker, S. M. Anthony, J.-N. Desrosiers, C. Senanayake, N. K. Garg, *Angew. Chem. Int. Ed.* **2016**, *55*, 15129 – 15132; *Angew. Chem.* **2016**, *128*, 15353 – 15356.
[20] Y. Bourne-Branchu, C. Gosmini, G. Danoun, *Chem. Eur. J.* **2017**, *23*, 10043 – 10047.
[21] For recent reviews for C–N bond cleavage reaction of amides through oxidative addition to metal complexes, see: a) G. Meng, S. Shi, M. Szostak, *Synlett* **2016**, *27*, 2530 – 2540; b) J. E. Dander, N. K. Garg, *ACS Catal.* **2017**, *7*, 1413 – 1423; c) S. Adachi, N. Kumagai, M. Shibasaki, *Tetrahedron Lett.* **2018**, *59*, 1147 – 1158; d) G. Meng, M. Szostak, *Eur. J. Org. Chem.* **2018**, 2352 – 2365.
[22] Y. Nishii, S. Akiyama, Y. Kita, K. Mashima, *Synlett* **2015**, *26*, 1831 – 1834.
[23] Y. Nishii, T. Hirai, S. Fernandez, P. Knochel, K. Mashima, *Eur. J. Org. Chem.* **2017**, 5010 – 5014.
[24] X. Chen, S. Hu, R. Chen, J. Wang, M. Wu, H. Guo, S. Sun, *RSC Adv.* **2018**, *8*, 4571 – 4576.
[25] T. Toyao, M. N. Rashed, Y. Morita, T. Kamichi, S. M. A. H. Siddiki, M. A. Ali, A. S. Touchy, K. Kon, Z. Maeno, K. Yoshizawa, K. Shimizu, *ChemCatChem* **2019**, *11*, 449 – 457.
[26] M. N. Rashed, S. M. A. H. Siddiki, A. S. Touchy, M. A. R. Jamil, S. S. Poly, T. Toyano, Z. Maeno, K. Shimizu, *Chem. Eur. J.* **2019**, *25*, 10594 – 10605.
[27] For recent other examples for esterification of tertiary amides by C–N bond cleavage, see: a) K. Yamada, Y. Karuo, Y. Tsukada, M. Kunishima, *Chem. Eur. J.* **2016**, *22*, 14042 – 14047; b) S. Adachi, N. Kumagai, M. Shibasaki, *Chem. Sci.* **2017**, *8*, 85 – 90; c) G. Li, P. Lei, M. Szostak, *Org. Lett.* **2018**, *20*, 5622 – 5625; d) H. Wu, W. Guo, S. Daniel, Y. Li, C. Liu, Z. Zeng, *Chem. Eur. J.* **2018**, *24*, 3444 – 3447; e) D. Ye, Z. Liu, H. Chen, J. L. Sessler, C. Lei, *Org. Lett.* **2019**, *21*, 6888 – 6892.
[28] H. Nagae, T. Hirai, D. Kato, S. Soma, S. Akebi, K. Mashima, *Chem. Sci.* **2019**, *10*, 2860 – 2868.
[29] a) J. Burés, *Angew. Chem. Int. Ed.* **2016**, *55*, 16084 – 16087; *Angew. Chem.* **2016**, *128*, 16318 – 16321; b) J. Burés, *Angew. Chem. Int. Ed.* **2016**, *55*, 2028 – 2031; *Angew. Chem.* **2016**, *128*, 2068 – 2071.
[30] For reweiw, see: C. D.-T. Nielsen, J. Burés, *Chem. Sci.* **2019**, *10*, 348 – 353.
[31] A. E. King, B. L. Ryland, T. C. Brunold, S. S. Stahl, *Organometallics* **2012**, *31*, 7948 – 7957. For kinetic model, see the Supporting Information.
[32] See the Supporting Information for the details for the DFT calculations.

Manuscript received: March 25, 2020
Accepted manuscript online: April 28, 2020
Version of record online: ■■ ▮▮, 0000